

The effect of number of electrodes and diagnostic tool for monitoring the delamination of CFRP laminates by changes in electrical resistance

Akira Todoroki*

Department of Mechano-aerospace Engineering, Tokyo Institute of Technology, 2-12-1, Ohokayama, Meguro-ku, Tokyo 152-8552, Japan

Received 10 May 2000; received in revised form 20 March 2001; accepted 14 June 2001

Abstract

The present study employs an electric-resistance change method for the identification of delamination cracks. In this method, the appropriate number of electrodes for identifying delaminations is investigated, and the diagnostic tool for the inverse problems to identify the delamination crack location and size from the electric resistance changes is discussed. FEM analyses are conducted to obtain electric resistance changes due to delamination crack creation with three-, four- and five-electrode type specimens. By the use of artificial neural networks (ANNs), the required number of electrodes for the identification of delamination-crack location and size from the electric resistance changes is investigated. By comparison of the estimations with the ANNs and with the response surfaces (RS), a better diagnostic tool is discussed in detail. As a result, the five-electrode type specimen is shown to be better for identification, and use of the RS with quadratic polynomials is a better tool than ANNs for the identification of delamination-crack location and size using electric resistance change. © 2001 Elsevier Science Ltd. All rights reserved.

Keywords: Composite; Monitor; Delamination; Carbon-fibre/epoxy; Electric resistance; Diagnosis; Artificial neural network; Response surfaces

1. Introduction

Composite laminates have low delamination resistance, and the low resistance causes delamination cracks even under slight impacts. Since the delamination cracks are usually invisible or difficult to detect by visual inspections, the delamination causes low reliability for primary structures. In order to improve the low reliability, automatic systems for delamination identifications in-service are desired. A health monitoring system to detect the delamination cracks is one of the desired approaches for practical laminated composite structures.

One of the approaches for detecting delamination cracks in service is to embed fiber-optic strain sensors into laminated composite structures to measure the strain as proposed by Badcock and Fernando [1] and by Chang and Sirkis [2,3]. This approach, however, may cause reductions of static strength and/or fatigue strength as shown by Seo and Lee [4]. The approach is, moreover,

very expensive owing to the high cost of optical fiber sensors and sensing systems, and the method is difficult to adopt for existing structures. A new smart technology is required to identify the location and size of the delamination cracks.

In the present study, an electric-resistance-change method is employed to identify the internal delamination cracks. The resistance-change method does not require expensive instruments. Since the method adopts the carbon-fiber reinforcement itself as sensors for delamination detection, this method does not cause reduction of static strength or fatigue strength, and it is applicable to existing structures. Moreover, the electric-potential method does not cause an increase in weight. The electric-potential method has therefore been adopted by several researchers such as Irving and Thiagarajan [5] and Abry et al [6]. Wang and Chung [7] have reported that delamination was detected by changes in electrical resistance.

Todoroki et al. [8,9] have already experimentally investigated the applicability of the electric resistance-change method for measurements of delamination crack length of the edge cracks for delamination resistance tests. For practical composite structures, however,

* Tel./fax: +81-3-5734-3178..

E-mail address: atodorok@ginza.mes.titech.ac.jp

delamination cracks are usually inside cracks. The inside cracks were also experimentally detected by the electric resistance change method by Todoroki [10] using carbon-fibre/PEEK composites. In order to investigate the effect of orthotropic electric resistance on the delamination monitoring, Todoroki and Suzuki [11] have conducted several FEM analyses and discussion. Todoroki and Suzuki [11] have revealed that the laminated composites have very large orthotropic electric resistances by the comparisons of the FEM analysis with the experimental data. The other paper has revealed electrodes should be placed on the specimen surface to conduct electric current in 0° direction [12]. That prevents placements of large numbers of electrodes to detect delamination.

In the present study, the number of electrodes that is appropriate for identification of delamination location and size is investigated, and the appropriate diagnostic tools for the monitoring are discussed on the basis of the FEM analyses. The identification of the delamination location and size from the electric resistance changes is one of the inverse problems. In order to identify the delamination location and size using the electric-resistance-change method, at least more than two electrodes are required to solve the inverse problems. Three types of the composite laminated beams are adopted as specimens. These are the three-electrode type, the four-electrode type and the five-electrode type. By using the three types of specimens, electric resistance changes due to the creations of delamination cracks are computed with FEM, and the inverse problems to obtain the delamination location and size are solved by using artificial neural networks (ANNs). Appropriate number of electrodes is investigated by the analytical data by using ANNs, and the appropriate diagnostic method is discussed by comparing the results with the ANNs and the response surfaces (RS).

In the present study, the ANN and the response surface methodology (RSM) is employed as convenient tools for the inverse problems. The ANN adopted in the present study, is the well-known back-propagation multilayered neural network. The RSM adopts quadratic polynomials. The estimation performance of the both methods are compared and discussed in detail.

2. Principle of electric potential method of laminated composites

Carbon fiber has a high electric conductivity, and the polymer matrix of a carbon-fibre/polymer (CFRP) is insulation resistant. For ideal CFRP composites, electric resistance in fiber orientation is almost zero. The electric resistance of transverse orientation is ideally infinity.

Practical CFRP laminates, however, have finite electric resistance in all directions. Practical carbon fiber in a unidirectional ply is serpentine as shown in Fig. 1(a). The curved carbon fiber creates a large carbon-fiber

network produced by the fiber contacts in a ply. The fiber-contact network brings finite electric resistance in the transverse orientation. In the same way, the fiber-contact-network produces finite electric resistance even in the thickness orientation in a ply. The electric resistance in transverse direction is much larger than the electric resistance of fiber orientation. Todoroki and Suzuki [11] have revealed that the ratio of the electric conductivity between the transverse direction and the fiber direction (σ_{90}/σ_0) is approximately $\sigma_{90}/\sigma_0 = 10^{-1}$ by the comparisons of analytical results of the electric potential changes due to the delamination crack growth with experimental data, and also showed that the ratio of the electric conductivity between the thickness direction and the fiber direction (σ_τ/σ_0) is approximately 10^{-3} – 10^{-4} .

The electric resistance of the thickness direction is very high comparing with that the electric resistance of fiber orientation. This is because thin resin-rich interlamina is electrically insulating, and the interlayer impedes fiber-contact through plies. For ideal CFRP composites, electric resistance in the thickness orientation is infinite due to the resin rich interlamina. For practical CFRP composites, however, plies of CFRP prepreg are serpentine such as fiber in a ply as shown in Fig. 1(b). The curve of plies causes fiber contacts through plies and creates finite electric resistance in the thickness direction even for thick laminated CFRP composites. If a delamination crack starts growing in the resin-rich interlamina, the crack breaks the fiber-contact-network between plies. The breakage of the contact network causes increase of the electric resistance of the graphite/polymer laminated composites. Therefore, delamination crack can be detected by the electric resistance change of a CFPR composite laminates.

3. Analytical method and specimen types

FEM analysis is employed for investigations of the effects of number of electrode and diagnostic tools in the present study. The FEM models used in the present

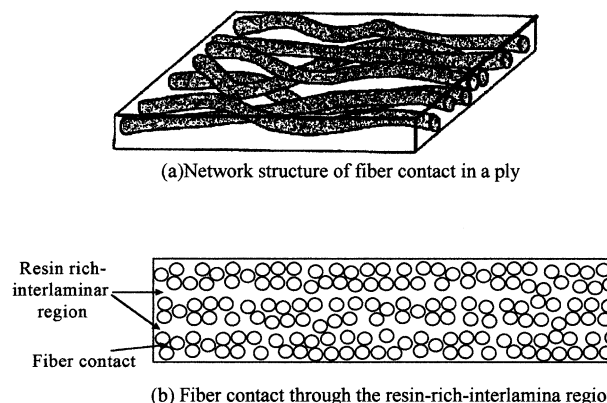
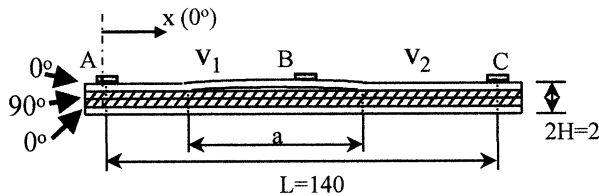


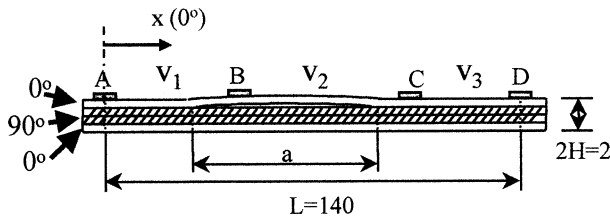
Fig. 1. Schema of practical fiber-contact of graphite/epoxy laminates.

study are shown in Fig. 2. Beam-type specimens are adopted for the analysis. The specimen length is $L = 140$ mm and thickness $2H = 2$ mm. Stacking sequence of the specimens is $[0_4/90_4]_s$. For the all type specimens (Fig. 2), all electrodes are mounted on the specimen top surface. The reason why all electrodes are mounted on the top surface is to identify delamination cracks from inside of the thin shell-type structures. The electrodes are mounted on the surface of the outermost ply of 0° plies. Authors have revealed that the electrodes should be placed on the 0° ply [12]. When the electrodes are placed on the 90° ply, the electric potential changes just above the delamination crack, and the electric resistance change is not measured between the electrodes. In the present study, therefore, all electrodes are placed on the specimen surface of the outermost ply of 0° plies.

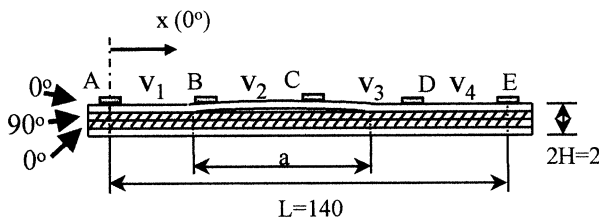
Delamination crack location is created between the two electrodes that locate both edges of the specimen. The delamination cracks, in the present study, locate near the surface where electrodes are mounted, and are created between the most inside 0° ply and the adjacent 90° ply. This is because delamination usually locates



(a) Three-electrode type specimen



(b) Four-electrode type specimen



(c) Five-electrode type specimen

Fig. 2. Specimen types.

near the reversed surface from the impacted surface for the thin laminates.

For the FEM analysis, inhomogeneous orthotropic carbon/epoxy composite material is regarded as the homogeneous orthotropic materials. The ratio of electric conductance between the 0° direction and 90° direction adopted here is $\sigma_{90}/\sigma_0 = 10^{-1}$, and the ratio between the 0° direction and thickness direction is $\sigma_t/\sigma_0 = 10^{-4}$. Four-node rectangular elements that have orthotropic electric conductivity were employed for the analysis. The size of the each element is approximately equal to 0.25 mm (approximately two-ply thickness). FEM analysis was conducted by using the FEM application program ANSYS. The effect of the resin-rich layer is regarded as very low homogeneous electric conductivity in the thickness direction for all elements. This could cause a small error in microscopic view of the size of one ply, but does not affect the macroscopic electric current. By using the auto-mesh-generation tool of ANSYS, the model was divided into approximately 6,000 two-dimensional elements. On the delamination crack surface lines, all nodes are doubly defined to represent crack surfaces. When a delamination crack grows, the doubly defined nodes on the delamination crack surfaces are released with each other to represent electric current insulation (Fig. 3).

For an orthotropic electric resistance field, direct electric current field is governed by the equation shown below.

$$J = (\sigma_x, \sigma_y) \begin{bmatrix} \frac{\partial \varphi}{\partial x} \\ \frac{\partial \varphi}{\partial y} \end{bmatrix} \quad (1)$$

$$\nabla \cdot J = 0 \quad (2)$$

where J is electric current density (A/m^2), σ_x and σ_y are electric conductance of the x -axis direction and y -axis direction (A/m), and φ is electric voltage (V). Eqs. (1) and (2) are the same as the thermal conduction equations for orthotropic thermal conductance field. Therefore, we can compute orthotropic electric resistance field by using the thermal conduction equation analysis of ANSYS.

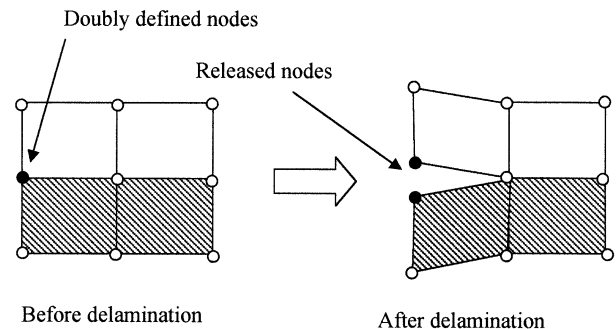


Fig. 3. Modeling of delamination progress.

For all types of the specimens, electric resistance changes between two adjacent electrodes are computed after the creation of a delamination crack. For the FEM computations, direct electric current of 30 mA is applied to the one electrode and electric voltage at the other adjacent electrode is set to 0 V. The obtained electric resistance change ΔR is normalized by the initial electric resistance R_0 . The electric resistance change ratio $v = \Delta R/R_0$ is used in the present study.

In the present study, total number of the computation cases is 54. The delamination locations computed in the present study are from 5 to 135 mm, and the size is 10, 20, 40, 60 and 80 mm. From the 54 results, 49 cases are randomly selected for training data sets for diagnostic tools. The remaining five cases are used to check the performance of approximations for the new data that are not used for training.

4. Diagnostics tools

4.1. Artificial neural networks

Identification of delamination location and size from the measured electric resistance change ratio is an inverse problem. In the present study, many data sets of electric resistance change ratio after the delamination creation are obtained from the FEM analyses. These data sets are applicable for training of ANNs. In the present study, a well-known three-layer-back-propagation network is adopted as one of the tools for the inverse problems. The three-layer-back-propagation ANN is schematically shown in Fig. 4.

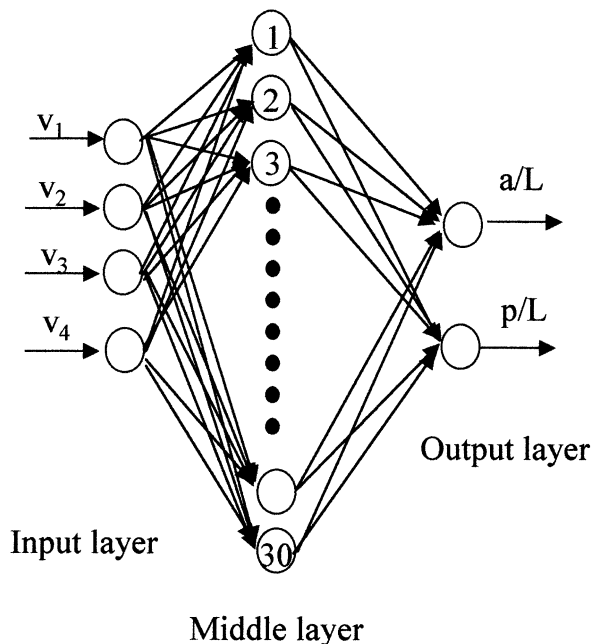


Fig. 4. Artificial neural network structure.

For the ANN, the input information is the electric resistance ratio, and the output information is the normalized delamination size (a/L) and location (p/L). The delamination location is defined at the coordinate of the delamination crack center, and it is normalized by the specimen length L . The number of neurons in the input layer equals the number of electric resistance ratio that is less than the number of electrodes by one. The number of neurons in the middle layer is 30, and the number was decided by the trial and error computations. The output information is the normalized delamination size and location, and the number of the neurons of the output layer is two. The all-link values among the neurons are set on the basis of random numbers, and the link values are corrected to obtain the least square errors with a back propagation training method. For the training of the neural networks, the moment method is adopted to obtain better training performance. The correction of the each link value $W_{i,j}$ is defined as follows.

$$W_{i,j \rightarrow i+1,k}(t+1) = W_{i,j \rightarrow i+1,k}(t) + (1 - \alpha)\Delta_{i,j \rightarrow i+1,k}(t+1) + \alpha\Delta_{i,j \rightarrow i+1,k}(t) \quad (3)$$

where t is the training cycle number, i is the layer number, j is the neuron number in the layer number of i , and k is the neuron number of the layer number of $i+1$. $W_{i,j \rightarrow i+1,k}$ is the link value from the neuron number j in the layer number i to the neuron number k in the layer number $i+1$. $\Delta_{i,j \rightarrow i+1,k}$ is the correction value calculated from the derivation of the sigmoid function and output error. α is the momentum term. In the present study, α is set to 0.5. The error $\Delta_{i,j \rightarrow i+1,k}$ is calculated, and the correction of each link value is conducted using Eq. (3) by each training data. Since the detail of the back-propagation neural network has already published in some textbooks, the detail is omitted here [13].

4.2. Response surfaces

The RS methodology is a widely adopted tool for quality engineering fields [14]. The response surface methodology comprises regression surface fitting to obtain approximated responses, design of experiments to obtain minimum variances of the responses and optimizations using the approximated responses.

For the present study, estimation of delamination locations and sizes from measured electric resistance change ratios is one of the inverse problems. In the present study, the RSM is adopted as a solver of inverse problems. The RSM gives three advantages for the problems. One of the advantages of using RSM is that the inverse problems can be approximately solved without modeling of the electric resistance change as the same as the case with ANN. The second advantage is that the performances of the approximated RS can be evaluated using statistical tools. The last advantage is that the minimum variances of the

response surfaces can be obtained using design of experiments with the small number of experiments.

For most of the RS, the functions for the approximations are polynomials because of simplicity, although the function of the response surface is not limited to the polynomials. For the cases of quadratic polynomials, the response surface is described as follows.

$$y = \beta_0 + \sum_{j=1}^k \beta_j x_j + \sum_{j=1}^k \beta_{jj} x_j^2 + \sum_{i=1}^{k-1} \sum_{j=i+1}^k \beta_{ij} x_i x_j \quad (4)$$

where k is the number of variables. In the case of two variables, the response surface is expressed as follows.

$$y = \beta_0 + \beta_1 x_1 + \beta_2 x_2 + \beta_3 x_1^2 + \beta_4 x_2^2 + \beta_5 x_1 x_2 \quad (5)$$

By replacements of $x_3 = x_1^2$, $x_4 = x_2^2$, $x_5 = x_1 x_2$, Eq. (4) becomes a linear regression model.

$$y = \beta_0 + \beta_1 x_1 + \beta_2 x_2 + \beta_3 x_3 + \beta_4 x_4 + \beta_5 x_5 \quad (6)$$

In the case that total number of experiments is n , the response surface can be expressed as follows using matrix expression.

$$\mathbf{Y} = \mathbf{X}\boldsymbol{\beta} + \boldsymbol{\varepsilon} \quad (7)$$

where

$$\mathbf{Y} = \begin{Bmatrix} y_1 \\ y_2 \\ \vdots \\ y_n \end{Bmatrix} \quad \mathbf{X} = \begin{bmatrix} 1 & x_{11} & x_{12} & \dots & x_{1k} \\ 1 & x_{21} & x_{22} & \dots & x_{2k} \\ \vdots & \vdots & \vdots & \ddots & \vdots \\ 1 & x_{n1} & x_{n2} & \dots & x_{nk} \end{bmatrix}$$

$$\boldsymbol{\beta} = \begin{Bmatrix} \beta_0 \\ \beta_1 \\ \vdots \\ \beta_k \end{Bmatrix} \quad \boldsymbol{\varepsilon} = \begin{Bmatrix} \varepsilon_1 \\ \varepsilon_2 \\ \vdots \\ \varepsilon_n \end{Bmatrix}$$

where $\boldsymbol{\varepsilon}$ is an error vector.

The unbiased estimator \mathbf{b} of the coefficient vector $\boldsymbol{\beta}$ is obtained using the well-known least square method as follows.

$$\mathbf{b} = (\mathbf{X}^T \mathbf{X})^{-1} \mathbf{X}^T \mathbf{Y} \quad (8)$$

The variance–covariance matrix of the \mathbf{b} is obtained as follows.

$$\text{cov}(b_i, b_j) = C_{ij} = \sigma^2 (\mathbf{X}^T \mathbf{X})^{-1} \quad (9)$$

where the σ is the error of \mathbf{Y} . The estimated value of σ is obtained as follows.

$$\sigma^2 = \frac{\text{SS}_E}{n - k - 1} \quad (10)$$

SS_E is a square sum of errors, and expressed as follows.

$$\text{SS}_E = \mathbf{Y}^T \mathbf{Y} - \mathbf{b}^T \mathbf{X}^T \mathbf{Y} \quad (11)$$

In order to judge the performance of the approximation of the RS, the adjusted coefficient of multiple determination R_{adj}^2 (R-square-adjusted) is used.

$$R_{\text{adj}}^2 = 1 - \frac{\text{SS}_E / (n - k - 1)}{S_{yy} / (n - 1)} \quad (12)$$

where S_{yy} is the total sum of squares.

$$S_{yy} = \mathbf{Y}^T \mathbf{Y} - \frac{(\sum_{i=1}^n y_i)^2}{n} \quad (13)$$

Each coefficient of the response surface can be tested by using t -statistic. The t -statistic of the coefficient b_j is expressed as follows.

$$t_0 = \frac{b_j}{\sqrt{\sigma^2 C_{jj}}} \quad (14)$$

where the C_{jj} is the element of number jj of variance–covariance matrix of Eq. (9).

Design of experiments is applied to reduce the variant of each coefficients in the approximated responses. Eq. (9) tells that reduction of the $(\mathbf{X}^T \mathbf{X})^{-1}$ makes relatively reduced variant without using the σ^2 that depends on the response y . Appropriate selections of the points for experiments can cause the reduced variants of the coefficients. The selection of the points for experiments to reduce the $(\mathbf{X}^T \mathbf{X})^{-1}$ is called design of experiments (DOE). For the practical DOE of quality engineerings, orthotropic designs or central composite designs are usually adopted. In the present study, full factorial design is adopted because the FEM analysis of this model does not require high computational cost. Therefore, DOE is not mentioned here.

Measured electric resistance change ratio data of multiple segments between electrodes (from v_1 to v_4) are variables, and the delamination location and size are the responses in the present study. In the present study, quadratic polynomials are adopted as RS function because of simplicity. In order to estimate delamination location, two separated RS are produced.

5. Results and discussion

5.1. Effect of number of electrodes

The FEM results obtained from the three-electrode-type specimen are shown in Fig. 5. In the figure, the

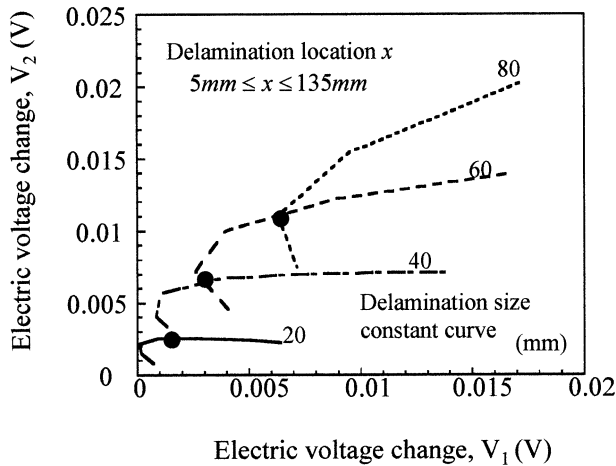


Fig. 5. Resistance change of AB and BC of various types of delamination location and size in the case of three-electrode type specimen.

abscissa is the electric resistance change ratio V_1 between the electrode A and B, and the ordinate is the electric resistance change ratio V_2 between the electrode B and C. Four cases of delamination size of various delamination locations are computed and shown in the figure. As you can see, there are cross points among the results of the different delamination size. The cross points in the figure imply that the electric resistance change ratios of the different delamination size are the same as each other.

In order to investigate the reason of the cross points, the electric current density of the specimen is investigated. Fig. 6 shows the results of the electric current density without delamination crack in the direction of the x axis (D_x) at the cross section of $x=110$ mm. Electric current is charged between the electrode A and B. In this case, direct current of 30 mA is charged to the

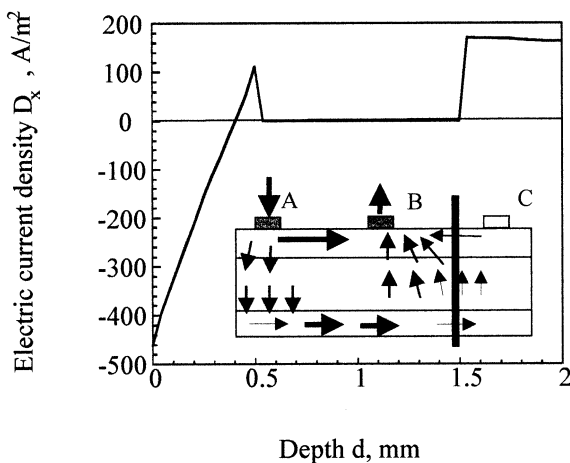


Fig. 6. Electric current density at the cross-section between the electrode B and C when the electric current is charged between A and B (A: 30 mA, B: 0 V).

electrode A, and the electric voltage of the electrode B is kept to 0 V. The electric current shown in the figure is at the cross section between the electrode B and C. The abscissa is the distance from the specimen top surface where the electrodes are mounted, and the ordinate is the electric current density. As shown in this figure, some part of the electric current flows in the segment between electrodes that are not charged as shown schematically. The electric current flows in the positive direction in the specimen bottom, and the current near the electrodes flows in the negative direction (negative electric current density). This difference of flow directions means that the circular flow is created in the adjacent non-charged segment to the charged segment.

When the delamination crack is created in a segment, the electric resistance changes in the delaminated segment. The circular electric current in the adjacent segment causes electric resistance change of the adjacent non-delaminated segment. Therefore, the electric resistance change due to a large delamination crack in the adjacent segment is equal to that due to a small delamination crack in the charged segment. This causes some cross points in Fig. 5. The cross points means that the diagnosis is impossible when only three electrodes are mounted on the laminates.

The delamination location and size can be identified from the electric resistance changes for the four-electrode type specimens and the five-electrode type specimens. Fifty-four cases of the different delaminations were calculated to obtain data for training and checking performance of the ANNs. The ANNs were trained using 49 cases, and the performance of the diagnosis of the ANNs for the new data was tested using the remaining five cases. In all ANNs, trainings were conducted until 10^6 cycles of training.

The results of the diagnosis of the four-electrode specimen are shown in Fig. 7(a) and (b). The results of the diagnosis of the five-electrode specimen are shown in Fig. 8(a) and (b). The results of the diagnosis of the delamination location are Fig. 7(a) and Fig. 8(a), and the results of delamination size are Fig. 7(b) and Fig. 8(b), respectively. In all figures, the abscissas are values of delamination location and size of the FEM models, and the ordinates are estimated results. The open symbols are estimated results data used for training, and the solid symbols are estimated results for the new data that are not used for training.

Figs. 7 and 8 show that the ANNs may estimate exact location and size of the delamination for both types of the specimens for the data used for training. However, the solid symbols represent that the results of the new data that are not used for training are unallowable poor estimations. These large estimation errors for the new data are usually observed for ANN of the over-training. The over-training means that the number of training cycles is too large. When the over-training occurs, the

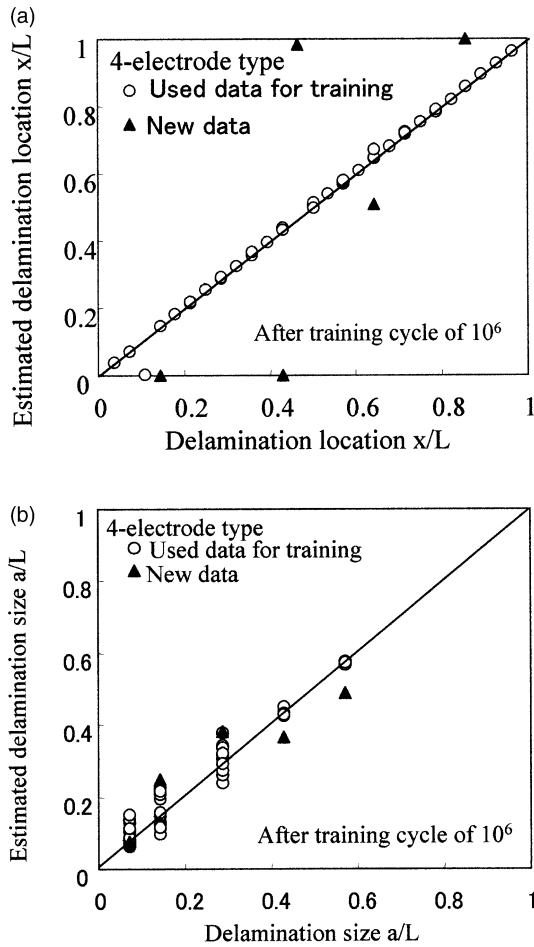


Fig. 7. Delamination identification estimation by artificial neural networks with a 4-electrode type specimen.

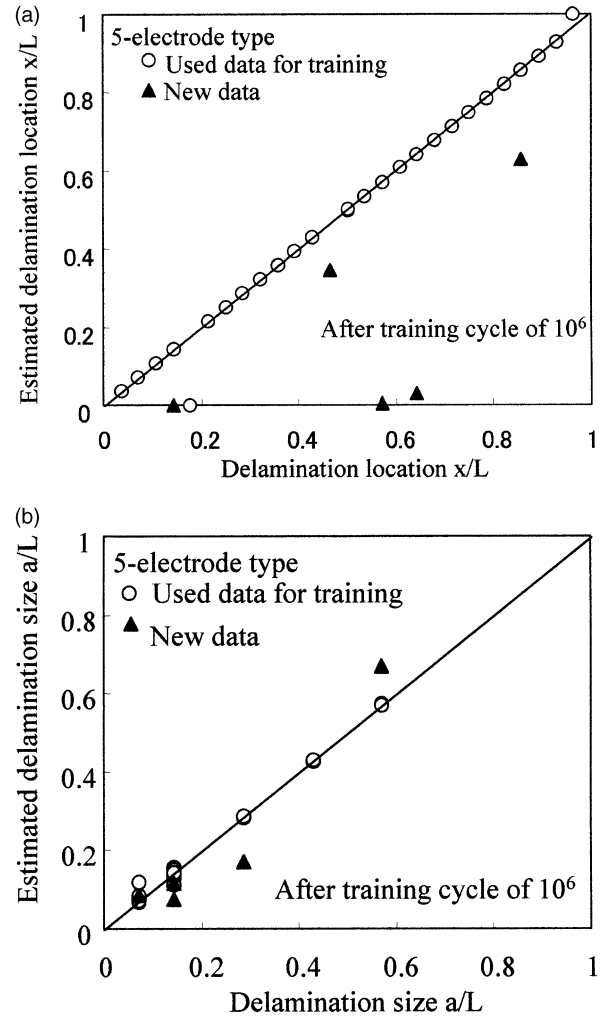


Fig. 8. Delamination identification estimation by artificial neural networks with a 5-electrode type specimen.

neural network provides significant error for the slight change of the input data. Usually, the over-training is prevented by terminating the training process before the neural network provides small errors for the training data. The process is defined under-training here. This is discussed in the next section.

Training processes of the decrease of estimation error for each type of the specimen is compared and shown in Fig. 9 to investigate the appropriate number of electrodes for identifications of delaminations. In this figure, the abscissa is the number of training cycle, and the ordinate is the total sum of errors of all training data at each training process. Since the training process of the ANNs is on the basis of the initial random numbers, the total sum of the errors is the averaged results of five runs by changing seeds of random numbers. The total sum of errors of the four-electrode type specimen is always larger than that of the five-electrode type specimen as shown in the figure. Although both of the error decreases with the increase of the training cycles, the error of the five-electrode type specimen is always very small. The small error means low computational costs for training

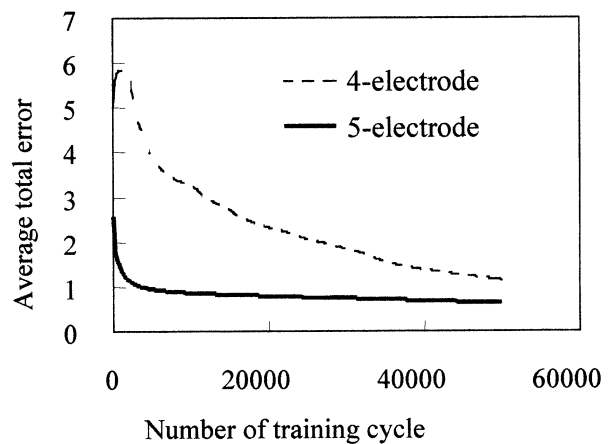


Fig. 9. Neural network training ratio.

and high performance with small runs of training. The results imply that the five-electrode type specimen is appropriate for practical training of ANNs for diagnosis of delaminations.

5.2. Comparison of diagnostic tools

Although the over-training of the ANNs may provide unallowable poor estimations, for practical delamination monitoring however, we cannot conduct a large number of runs of computations or experiments for investigations of performance for the new data. The most important advantages for the diagnostic tool of the structural health monitoring is to provide allowable estimations even for the new data. The advantages of the ANNs as the diagnostic tool must be clarified through investigations of the performances for the new data. Usually, the over-training problems can be avoided with an under-trained ANNs that is produced by terminating the training process before finishing. In addition, RS is proposed as a new diagnostic tool for structural health monitoring and the performance of the RS for the new data is compared and discussed. In this section, the under-trained ANN and the RS are compared as diagnostic tools.

Fig. 10 shows the estimation results of the delamination location with the under-trained ANN after fifty thousand training cycles. The abscissa and the ordinate are the same as those of the previous figures. Fig. 11 shows the estimation results of the delamination location of the under-trained ANN after a hundred thousand training cycles. From these figures, it seems that the training of these ANNs is incomplete because the estimation errors of the data for the training are still very large. For these under-trained ANNs, the ANNs estimate exactly for the part of the data used for training. On the other hand, the ANNs give poor estimations for other part of the data. For the new data, the estimations are not worse than the results of the over-trained ANNs, but there are still large errors in some estimations. For the under-trained ANNs, the differences between good

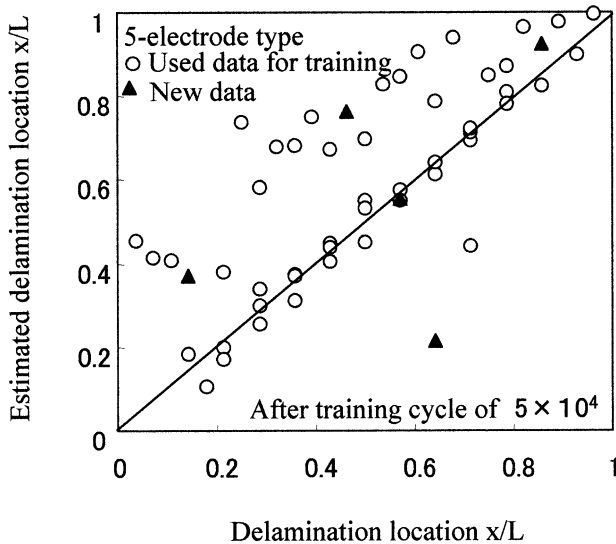


Fig. 10. Delamination location estimation by an under-trained artificial neural network.

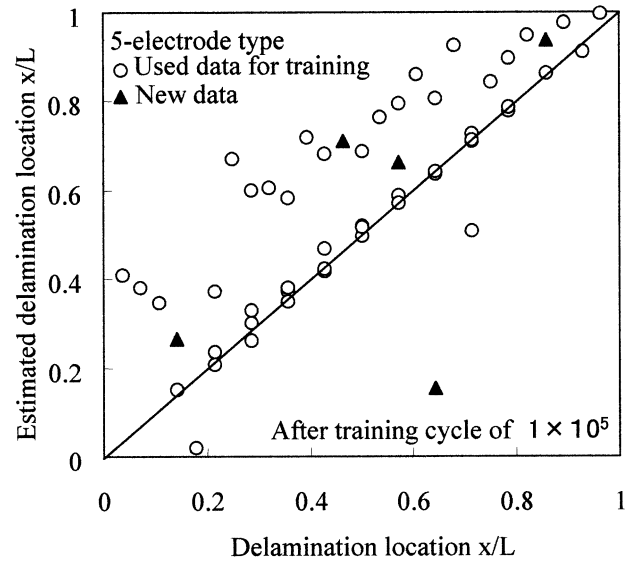


Fig. 11. Delamination location estimation by an under-trained artificial neural network.

estimations and poor estimations are very large. This means that the ANNs have a dangerous possibility of giving poor estimations for the new data even for the under-trained ANNs.

From the same 49 data, the RSs estimation of delamination location and size for five-electrode type specimen was calculated with the least square error method. Using the decreasing method, the terms that worsen R_{adj}^2 were deleted using t -statistics. The R_{adj}^2 of the RS for estimations of delamination location is 0.59, and the root mean square error is 0.155. The RS is as follows.

$$\begin{aligned} \frac{p}{L} = & 0.4867 - 8.814617v_1 + 3.0634381v_2 - 4.135599v_3 \\ & - 3.786172v_4 + 26.05818v_1^2 - 15.95931v_1v_2 \\ & + 41.570858v_1v_3 - 8.119241v_2v_3 - 85.74348v_1v_4 \\ & + 29.027751v_2v_4 - 10.07303v_3v_4 \end{aligned} \quad (15)$$

where v_i ($i=1, \dots, 4$) is the electric resistance change of each segment magnified by the factor of 10^2 .

In the same way, the RS estimation of size was obtained. The R_{adj}^2 of the RS for estimations of delamination location is 0.967, and the root mean square error is 0.0318. The RS is as follows.

$$\begin{aligned} \frac{a}{L} = & 0.0521 + 0.9268609v_1 - 0.034172v_2 + 0.1986073v_3 \\ & + 0.6646841v_4 + 2.1459641v_2^2 + 2.9375724v_3^2 \\ & + 5.3316345v_4^2 - 3.588444v_1v_2 - 2.380592v_1v_3 \\ & - 2.906398v_2v_3 + 15.540179v_1v_4 - 8.16004v_3v_4 \end{aligned} \quad (16)$$

Fig. 12 shows the results of estimations of delamination location with RS. Fig. 13 shows the results of the

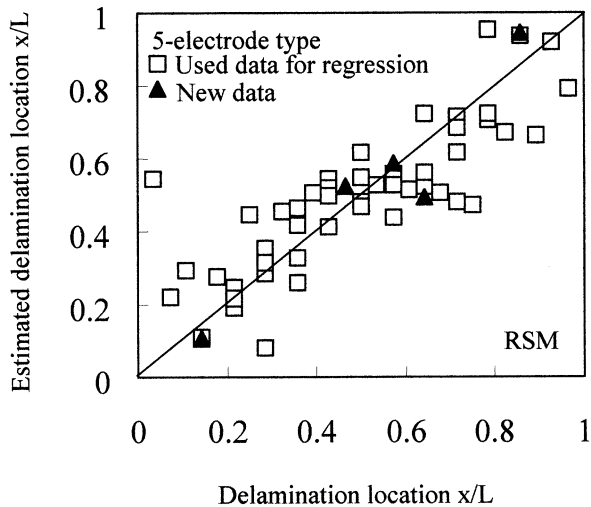


Fig. 12. Delamination location estimation by response surface methodology.

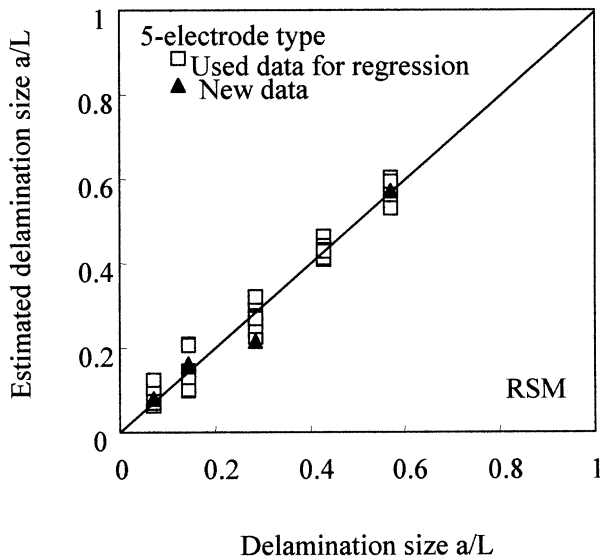


Fig. 13. Delamination size estimation by response surface methodology.

estimations of delamination size with RS. The abscissas and ordinates of these figures are the same as those of ANNs. The open symbols are the estimations of the data used for regression, and the solid symbols are the estimations of the new data that are not used for regression. Although the RSM has employed simple quadratic polynomials for the functions of approximations, the RSs may give good estimations. The RSM does not give poor estimations even for the new data that are not used for regression.

The estimation performance for the new data of both tools can be compared using the square sum of errors of the estimations of the ANNs and the RSs for the new data. The square sum of errors of the new five data (S_{SE5}) for the RS to estimate delamination location is only 0.035. On the other hand, the S_{SE5} for the over-trained

ANN is 0.786, and the both values of the S_{SE5} for the both of the under-trained ANNs are 0.33. The decrease of the S_{SE5} by the employment of the less cycles of training for the ANN means that the under-trained ANN provides the better approximations for the new data compared with the over-trained ANNs. The RSM gives the best results for the estimation for the new data.

The ANNs require many tuning processes such as training parameters or network structures to obtain better estimations, as it is generally known. Even after the tunings, the ANNs may not always provide good estimations for the new data as shown in Figs. 7, 8, 10, and 11. This means that the ANNs are very difficult to handle for the tool of the diagnosis to identify delaminations. The problem of the ANNs could be improved by some modifications. For example, the ANNs in the present study employ the training rule that the link values of the ANNs are modified by the each training data, and this may cause many local minimums of the link values. More runs of searches could bring better ANNs because the ANNs depend on the random numbers. However, the improvements may not release us from the difficult tuning of ANNs.

The RSM does not have the problem of the tuning, and we can easily estimate the performance of the RS by using the statistical tools for the data used for the regression. For the RSs in Eqs. (15) and (16), the first-order interaction terms contribute important roles more than the square terms for the regression, because the absolute value of t -statistics of the term of v_1^2 is only 1.92 but the absolute value of t -statistics of the other interaction terms are larger than 2.78. This implies that the inverse problem of the diagnosis to identify delaminations do not include higher order terms, and the high R_{adj}^2 with the simple polynomials means that the identification of delamination location and size from the electric resistance change is the relatively simple problem as an inverse problem. This simplicity may bring high reliability for the new data with RS, however, we can employ multiple response surfaces for divided spaces with strong statistical tools even if we have complicated problems and low R_{adj}^2 of the RS. Thus, it can be concluded that the RSM has high potential for a diagnostic tool for delamination monitoring using electric resistance change.

6. Conclusions

In the present study, FEM analyses were conducted to obtain electric resistance changes due to delamination crack creations. Using the ANNs, the required number of electrodes for identifications of delamination cracks location and size from the electric resistance changes was investigated. By comparisons of the estimations with the ANN and with the RSM, better diagnostic tool is investigated in detail. The results obtained are as follows:

1. the three-electrode type specimen cannot identify the delamination crack location and size due to the large difference of the electric resistances between fiber direction and thickness direction;
2. the five-electrode type specimen is appropriate for identifications of delaminations; and
3. the RSM using quadratic polynomials is better than the ANN as a diagnostic tool for identifications of delamination using electric resistance change.

References

- [1] Badcock RA, Fernando GF. An intensity-based optical fibre sensor for fatigue damage detection in advanced fibre-reinforced composites. *Smart Materials and Structures* 1995;4:223–30.
- [2] Chang C-C, Sirkis J. Impact-induced damage of laminated graphite/epoxy composites monitoring using embedded in-line fiber etalon optic sensors. *Journal of Intelligent Material Systems and Structures* 1997;8:829–41.
- [3] Chang C-C, Sirkis JS. Design of fiber optic sensor systems for low velocity impact detection. *Smart Materials and Structures* 1998;7:166–77.
- [4] Seo DC, Lee JJ. Effect of embedded optical fiber sensors on transverse crack spacing of smart composite structures. *Composite Structures* 1995;32:51–8.
- [5] Irving PE, Thiagarajan C. Fatigue damage characterization in carbon fibre composite materials using an electric potential technique. *Smart Materials and Structures* 1998;7:456–66.
- [6] Abry JC, Bochart S, Chateauminois A, Salvia M, Giraud G. In situ detection of damage in CFRP laminates by electric resistance measurements. *Composite Science and Technology* 1999;59:925–35.
- [7] Wang X, Chung DDL. Sensing delamination in a carbon fiber polymer-matrix composite during fatigue by electrical resistance measurement. *Polymer Composite* 1997;18-6:692–700.
- [8] Todoroki A, Matsuura K, Kobayashi H. Application of electric potential method to smart composite structures for detecting delamination. *JSME International J, Series A* 1995;38(4):524–30.
- [9] Todoroki A, Kobayashi H, Matsuura K. Application of electrical potential method as delamination sensor for smart structures of graphite/epoxy. In: Inoue K, Shen SIY, Taya M, editors. US–Japan workshop on smart materials and structures. University of Washington: TMS, 1997. p. 47–54.
- [10] Todoroki A. Delamination detection by electric resistance change for graphite/PEEK composites. *Proceedings of the 5th Japan International SAMPE Symposium* 1997:899–904.
- [11] Todoroki A, Suzuki H. Evaluation of orthotropic electrical resistance for delamination smart detection of graphite/epoxy composites by electrical potential method. *Proceedings of 1st Asian-Australian Conference on Composite Materials (ACCM-1)* 1998:630–1.
- [12] Todoroki A, Suzuki H. Health monitoring of internal delamination cracks for graphite/epoxy composites by electric potential method. *Applied Mechanics and Engineering* 2000;5-1:283–94.
- [13] Rogers J. *Object-oriented neural networks in C++*. Academic Press, San Diego, CA, USA, 1997.
- [14] Myers RH, Montgomery DC. *Response surface methodology: process and product optimization using designed experiments*. John Wiley, New York, NY, USA, 1995.